DMD Fast Forward. Published on February 19, 2014 as doi:10.1124/dmd.114.057042

DMD #57042

Inhibition of SULT4A1 expression induces up-regulation of phototransduction gene expression in 72 hours post fertilization zebrafish larvae.

Frank Crittenden, Holly Thomas, Cheryl M Ethen, Zhengliang L Wu, Dongquan Chen, Timothy Kraft, John Parant, and Charles N Falany

Department of Pharmacology and Toxicology, University of Alabama at Birmingham, Birmingham, AL. (F.C., H.T, J.P., C.N.F.)

R&D Systems, 614 McKinley Place NE, Minneapolis, MN. (C.M.E, Z.L.W.)

Department of Medicine, University of Alabama at Birmingham, Birmingham, AL. (D.C.)

Department of Vision Sciences, University of Alabama at Birmingham, Birmingham, AL. (T.K.)

DMD Fast Forward. Published on February 19, 2014 as DOI: 10.1124/dmd.114.057042
This article has not been copyedited and formatted. The final version may differ from this version.

DMD #57042

Running title: SULT4A1 knockdown up-regulates phototransduction proteins

Corresponding Author:

Charles N Falany, Ph.D

Volker Hall 151

Department of Pharmacology and Toxicology

University of Alabama at Birmingham

1670 University Blvd

Birmingham AL, 35294

Telephone: 205 934 9848

Fax: 205 934 8240

Email: Cfalany@uab.edu

Number of text pages: 14

Number of tables: 3

Number of figures: 4

Number of references: 27

Number of words in the Abstract: 172

Number of words in the introduction: 480

Number of words in the discussion: 1309

Abbreviations: BR-STL – brain sulfotransferase-like protein; FDR – false discovery rate; grk1b – G protein-coupled receptor kinase 1b; guca1e – guanylate cyclase activator 1e; KD – knockdown; MO – morpholino oligonucleotide; OPN1MW1 – opsin 1, medium-wave-sensitive, 1; PAP – 3',5'-phosphoadenosine; PAPS – 3'phosphoadenosine-5'-phosphosulfate; PBS – phosphate buffered saline; qPCR – quantitative PCR; RNA-seq – deep RNA-sequencing; RPKM – reads per kilobase of exon model per million mapped reads; rrh – retinal pigment epithelium-derived rhodopsin homologue; SCM – Standard control morpholino; SULT – sulfotransferase; WT – wild type

ABSTRACT

Sulfotransferase (SULT) 4A1 is an orphan enzyme that shares distinct structure and sequence similarities with other cytosolic SULTs. SULT4A1 is primarily expressed in neuronal tissue and is also the most conserved SULT, having been identified in every vertebrate investigated to date. Certain haplotypes of the SULT4A1 gene are correlated with higher baseline psychopathology in schizophrenic patients, but no substrate or function for SULT4A1 has yet been identified despite its high level of sequence conservation. In this study, RNA-seq was used to search for alterations in gene expression in 72 hours post fertilization (hpf) zebrafish larvae following transient SULT4A1 knockdown (KD) utilizing splice blocking morpholino oligonucleotides (MOs). This study demonstrates that transient inhibition of SULT4A1 expression in developing zebrafish larvae results in the up-regulation of several genes involved in phototransduction. SULT4A1 KD was verified by immunoblot analysis and quantitative real-time PCR (qPCR). Gene regulation changes identified by deep RNA sequencing were validated by qPCR. This study is the first identification of a cellular process whose regulation appears to be associated with SULT4A1 expression.

INTRODUCTION

Sulfotransferase (SULT) 4A1 was first identified, molecularly cloned, and expressed in 2000 by Falany *et al* from the brains of humans and rats (Falany, 2000). The protein was initially named "brain sulfotransferase-like protein" (BR-STL) because of sequence similarity to the cytosolic SULTs and a lack of identifiable SULT activity. However, the protein was later renamed SULT4A1 based on sequence and structural homologies to other cytosolic SULTs (Liyou, 2003; Blanchard, 2004). SULTs are a superfamily of enzymes responsible for the sulfonation of a wide variety of compounds, both endogenous and exogenous. The SULTs catalyze a Phase II conjugation reaction in which a sulfonate group is transferred from the obligate donor, 3'-phosphoadenosine-5'-phosphosulfate (PAPS), onto the hydroxyl group of an acceptor substrate to form a sulfate. Addition of the charged sulfonate group generally renders the substrate more water soluble and increases excretion. Key structural features shared between SULT4A1 and other SULTs include the KXXFTVXXXE dimerization domain, active site histidine, and PAPS binding site (Falany, 2000).

SULT4A1 is the most conserved of all of the SULTs, suggesting an important and conserved function. That function or enzymatic activity, however, has yet to be elucidated. Unlike other SULTs, SULT4A1 is exclusively expressed in neural tissue (Falany, 2000; Liyou, 2003). Moreover, recent evidence suggests that a specific SNP haplotype in the 5' untranslated region of the SULT4A1 gene is correlated with higher baseline psychopathology in patients with schizophrenia and is predictive of those patients' responses to treatment with olanzapine (Ramsey, 2011). However, a mechanism for the role of SULT4A1 in the pathology of schizophrenia has not been described.

The use of zebrafish (*Danio rerio*) as a model organism offers a unique opportunity to gain insight into the activity or function of SULT4A1. To date, 16 SULT genes have been identified in and cloned from zebrafish (Liu, 2010). Like all other vertebrate forms of SULT4A1, zebrafish SULT4A1

(zfSULT4A1) and human SULT4A1 (hSULT4A1) exhibit extensive amino acid sequence homology (86.97% identity and 91.9% similarity). SULT4A1 is expressed almost exclusively in neuronal tissue, and the nervous system develops early in zebrafish larvae. In light of these facts, *D. rerio* is an excellent organism for the investigation of the regulation, localization, and function of SULT4A1. Furthermore, the ability to knockdown (KD) SULT4A1 expression in the developing zebrafish embryo using splice-blocking antisense morpholino oligonucleotides (MOs) may provide key insights into the function of this protein.

Previous studies have demonstrated the practicality of MOs as a means to knock-down gene expression in zebrafish larvae during the first few days of development (Draper, 2001). Given the rapid development of the zebrafish nervous system and the anticipated rapid onset of SULT4A1 expression, this ability provides an excellent opportunity to investigate a developmental response to the loss of SULT4A1 expression. This report describes the effect of SULT4A1 KD on the transcriptome of 72 hours post fertilization (hpf) zebrafish larvae as assessed by deep RNA-sequencing (RNA-seq) analysis.

MATERIALS AND METHODS

Zebrafish lines and maintenance

Tubingen and type AB zebrafish strains were housed in a recirculating aquaria system (Aquaneering Inc.) in the UAB Zebrafish Research Facility and cared for in accordance with the guidelines set forth by the Institutional Animal Care and Use Committee of the University of Alabama at Birmingham (IACUC APN: 09641).

Morpholino (MO) KD

MOs (Gene Tools) were designed to target the splice donor sites of exon 1 of the SULT4A1 transcript (SULT4A1 MO, 5'-TAATGCACGCGATTGAATACCTGAT-3'). This results in the inclusion of intron 1 in the transcript and an in-frame premature stop codon 382 bases downstream from the translation start site. MOs were reconstituted in deionized water and diluted to a working concentration of 1.64 mM. Embryos were collected from natural matings and injected using a Harvard Apparatus PLI-100 injection system at the one or two cell stage with 0.82 pmol of either SULT4A1 MO or a standard control MO (SCM, Gene Tools). Effectiveness of KD was verified by quantitative PCR (qPCR) using TaqMan Gene Expression Assays (Life Technologies). Zebrafish embryos injected with SULT4A1 MO and SCM were observed for gross morphological phenotype changes at 48, 72, and 120 hpf. At each time point, 10 SCM and 10 SULT4A1 MO embryos were selected at random and assessed for the development of heart, ears, eyes, circulatory system, and swim bladder.

Sample preparation and RNA-seq data analysis

Embryos injected with either SCM or SULT4A1 MO were separated into 4 groups of 15 embryos (2 SCM and 2 SULT4A1 MO). At 72 hpf, all 4 groups were sacrificed, and total RNA was isolated using STAT-60™ (Tel-Test). mRNA-sequencing was performed on an Illumina HiSeq2000 in the UAB Heflin

Center for Genomic Sciences. Briefly, the quality of the total RNA was assessed using the Agilent 2100 Bioanalyzer followed by 2 rounds of polyA+ selection and conversion to cDNA. TruSeq library generation kits were used as per the manufacturer's instructions (Illumina, San Diego, CA). Library construction consisted of random fragmentation of the polyA+ mRNA followed by cDNA production using random primers. The ends of the cDNA were repaired, A-tailed and adaptors ligated for indexing (up to 12 different barcodes per lane) during the sequencing runs. The cDNA libraries were quantitated using qPCR in a Roche LightCycler 480 with the Kapa Biosystems kit for library quantitation (Kapa Biosystems, Woburn, MA) prior to cluster generation. Clusters were generated to yield approximately 725K-825K clusters/mm2. Cluster density and quality were determined during the run after the first base addition parameters were assessed.

The raw FASTQ files were aligned to the zebrafish reference genome (Zv9, Sanger Institute) following workflow of Galaxy instance installed at UAB (http://galaxy.uabgrid.uab.edu). Pre-alignment was conducted to determine if trimming was needed based on reads quality score. The BAM files were generated following RNA-seq data analysis workflow of Tophat (Trapnell, 2009), Cufflinks, and Cuffcompare (Trapnell, 2010). These BAM files were loaded into Partek Genomics Suite 6.6 (Saint Louis, MO) for further statistical and functional analysis. Briefly, the reads per kilobase of exon model per million mapped reads (RPKM)-normalized reads (Mortazavi, 2008) were calculated and the expression levels of genes were estimated (Xing, 2006; Mortazavi, 2008; Wang, 2008). The differential expressions were determined by ANOVA as described in the vender user manual. A gene list was then created after false discovery rate (FDR) p-value correction using the Benjamini and Hochberg method (Benjamini and Hochberg, 1995). Further functional analysis was conducted using Ingenuity Pathway Analysis (IPA, Redwood City, CA).

DMD Fast Forward. Published on February 19, 2014 as DOI: 10.1124/dmd.114.057042
This article has not been copyedited and formatted. The final version may differ from this version.

Quantitative PCR

Embryos injected with either SCM or SULT4A1 MO were separated into 6 groups of 30 embryos (3 SCM and 3 SULT4A1 MO). At 72 hpf, all 6 groups were sacrificed, and total RNA was isolated using STAT-60™. RNA concentration was determined using a NanoDrop® ND-1000 spectrophotometer, and SuperScript III (Invitrogen) was used to generate complimentary DNA (cDNA) using 200 ng RNA from each sample. qPCR experiments comparing the following genes were carried out using pre-designed TaqMan Gene Expression Assays from Life Technologies with an Applied Biosystems™ 7900HT Sequence Detection System: SULT4A1, assay ID: Dr03078008_g1; retinal pigment epithelium-derived rhodopsin homolog (rrh), assay ID: Dr03108770_m1; G protein-coupled receptor kinase 1b (grk1b), assay ID: Dr03128502_m1; guanylate cyclase activator 1e (guca1e), assay ID: Dr03094375_m1; opsin 1, medium-wave-sensitive, 1 (opn1mw1), assay ID:Dr03079939_g1. Samples were compared using the ΔCt method, and p-values were determined using a one-tailed t-test. Statistical significance was assumed if the p-value was less than 0.05.

Adult type AB zebrafish were sacrificed; brain, eye, intestine, liver, and testes were dissected and flash frozen in liquid nitrogen. RNA was isolated, and cDNA was generated as described above. Relative SULT4A1 expression levels were determined for each tissue as described above (n=3). Conventional PCR using REDTaq™ DNA Polymerase (Sigma) and primers to generate full-length SULT4A1 (forward: 5'-atggcggaaagcgaggtgga-3'; reverse: 5'-ctgctttacaggataaagtc-3') was used in these tissues to verify the presence of full-length SULT4A1 mRNA

Immunoblot Analysis

Lysate was prepared from 72 hpf zebrafish embryos (KD and control) and adult zebrafish brain, eye, intestine, liver, and testes. Samples were dissected and placed in sterile phosphate-buffered saline (PBS) with Complete Mini EDTA-free Protease Inhibitor Cocktail Tablets (Roche) and Phosphatase Inhibitor Cocktail 2 (Sigma-Aldrich). Samples were disrupted by pipetting, vortexed 5 minutes at 4°C, and sonicated twice for 10 s with 30 s cooling on ice between sonications. The cycle of pipetting, vortexing, and sonicating was repeated, and lysate was collected by centrifugation at 15,000 x g for 20 min at 4°C. Immunoblot analyses were carried out using a goat polyclonal antibody raised to human SULT4A1 (R&D Systems). Lysate protein concentration was determined by Bradford analysis (Bradford 1976), and 396 µg total protein was loaded from each sample. SULT4A1 specificity was corroborated in each blot using an anti-human SULT4A1 mAb (R&D Systems). The polyclonal antibody was detected using a donkey anti-goat horseradish peroxidase-conjugated secondary (Santa Cruz). The monoclonal antibody was detected using a goat anti-mouse horseradish peroxidase-conjugated secondary (Southern Biotech). Both were developed with SuperSignal® West Chemiluminescent Substrate (Thermo Scientific) and exposed to autoradiograph film.

DMD Fast Forward. Published on February 19, 2014 as DOI: 10.1124/dmd.114.057042
This article has not been copyedited and formatted. The final version may differ from this version.

RESULTS

Sequence Conservation of SULT4A1 in D. rerio.

As observed with the other vertebrate SULT4A1 isoforms, zfSULT4A1 shares extensive homology with hSULT4A1. The two sequences are 87% identical and 92% similar. Although this is slightly lower conservation than is observed between hSULT4A1 and other terrestrial vertebrates (Table 1), it is still very high compared to the conservation between other cytosolic SULTs. Key conserved structural features that have resulted in the inclusion of SULT4A1 in the SULT gene family include the active site histidine (residue 111), the KXXFTVXXXE dimerization domain (residues 254-263), and the TYPKSGT sequence involved with PAPS binding (residues 52-58), which are all conserved in both hSULT4A1 and zSULT4A1. (Fig. 1)

SULT4A1 expression in brain and eye of adult zebrafish

The zfSULT4A1 gene is located on chromosome 9 and consists of 7 exons separated by 6 introns (ZDB-GENE-060421-2705). When qPCR was performed on cDNA from the brain, eye, intestine, liver, and testes of adult fish using a TaqMan® assay that spans the junction of exons 2 and 3, SULT4A1 mRNA was detected in the brain, eye, and testes (Fig. 2a). The findings in the brain and eye were corroborated by conventional PCR using primers to generate full-length SULT4A1. However, no SULT4A1 message was detected in cDNA of the testes when analyzed by conventional PCR to generate the SULT4A1 coding region and agarose gel separation (Fig. 2b).

After establishing SULT4A1 mRNA expression in the zebrafish brain and eye, immunoblot analyses were used to demonstrate that the SULT4A1 protein is detectable in these tissues. Immunoblot analysis using a goat polyclonal antibody of human SULT4A1 detected a band at approximately 33 kDa in lysate of both the brain and eye (Fig. 2c) corresponding to zSULT4A1 (MW = 33 kDa). As expected, no SULT4A1 was detected via immunoblot analysis in the testes lysate. Immunoblot analysis with the

polyclonal antibody to human SULT4A1 did detect SULT4A1 protein in control 72 hpf larvae lysate but not in SULT4A1 MO larvae (Fig. 2d).

SULT4A1 KD induced up-regulation of phototransduction genes.

To investigate the effects of the inhibited expression of SULT4A1, the gene expression profile of 72 hpf embryos injected with either SCM or SULT4A1 MO was assessed using RNA-seq. RNA-seq detects transcripts over a much larger dynamic range of expression compared to microarray technology (Wang 2009). Evaluation of the RNA-seq data using Ingenuity Pathway Analysis revealed a number of cellular processes to be significantly affected in the SULT4A1 KD larvae as compared to control larvae. A total of 135 messages were shown to be significantly dis-regulated by SULT4A1 KD. Of these, 47 genes were down-regulated, and 88 were up-regulated. A total of 13 genes known to be involved in phototransduction were dis-regulated by SULT4A1 KD, and all 13 of these affected genes were shown to be up-regulated (Table 2). Other pathways including LXR/RXR activation, circadian rhythm signaling, and CREB signaling in neurons were also affected by SULT4A1 KD, but none to the extent or significance of phototransduction (Table 3).

To validate the changes observed in the RNA-seq data, three up-regulated phototransduction genes were selected for further analysis by qPCR. OPN1MW1, guca1e, and grk1b were chosen based on their relative abundance, high observed fold-change, and p-value. Pre-designed TaqMan Gene Expression Assays were used to verify the observed up-regulation of OPN1MW1 ($p = 0.0047$) and grk1b ($p = 0.0392$). Guca1e showed an absolute increase of 1.52-fold when analyzed by qPCR, but this change was not statistically significant ($p = 0.0822$). As expected, SULT4A1 showed a significant 7-fold decrease in expression when analyzed by qPCR ($p = 0.0253$). Rrh was used as a negative control since it is

expressed in the retina and no change in expression levels was observed in the RNA-seq data. As expected, analysis by qPCR showed no significant change in rrh expression ($p = 0.3835$). (Fig. 3)

MO KD of SULT4A1 expression in developing zebrafish embryo

Although the SULT4A1 MO was effective at delaying SULT4A1 expression, no gross morphological phenotype was observed in SULT4A1 MO versus SCM – injected embryos (Fig. 4). At 48 hpf (fig. 4a and 4b), all observed SCM and KD embryos had a functional beating heart. At 72 hpf (fig. 4c and 4d), all observed SCM and KD embryos displayed adequate blood flow throughout the body. At 120 hpf (fig. 4e and 4f), all observed SCM and KD embryos had morphologically normal ears, eyes, and swim bladder.

DISCUSSION

The use of zebrafish as a model organism provides a unique opportunity to investigate the function of SULT4A1. Advantages of the zebrafish model include the fact that large numbers of KD larvae can be generated in a very short amount of time, and the rapid onset of SULT4A1 expression and nervous system development allows generation of specimens for *in vivo* study of SULT4A1 more rapidly than would be possible in other vertebrate model systems. Typically, the use of zebrafish to investigate the function of human proteins would carry the disadvantage that zebrafish are more distantly related to humans than other common model organisms. However, considering the highly conserved nature of SULT4A1's sequence and neural localization, results from zebrafish studies may have greater relevance to the analysis of hSULT4A1 function than with less conserved proteins. Because zfSULT4A1 and hSULT4A1 are highly conserved, it is anticipated that they have an equally conserved function. That function, once elucidated, will no doubt prove to generate novel insights into SULT function in nervous tissue.

qRT-PCR (Fig. 3a), immunoblot analysis (Fig. 2d), and RNA-seq (Table 2) showed an effective KD of SULT4A1 expression at 72 hpf. However, both the control and KD larvae developed normally, and no gross phenotypic changes could be observed. There are a number of possible explanations. If SULT4A1 is in fact an enzyme, then an incomplete KD, as is typically achieved with MOs, may leave sufficient levels of the protein to retain its function. Given the primarily neuronal expression of SULT4A1, it is also possible that a KD phenotype may manifest itself in the form of abnormal behavior patterns or neural activity rather than developmental pathogenesis. The correlation established by Ramsey *et al* (2011) between baseline schizophrenic psychopathology and a specific SULT4A1 haplotype lends credence to this possibility.

One unexpected finding of this study was the detection of SULT4A1 mRNA in the testes via qPCR (Fig. 2a). When full-length primers for SULT4A1 were used with cDNA from the testes, however, no amplification product was observed. Likewise, no translated protein was detected in the testis by immunoblot analysis. A similar phenomenon was observed in human liver by Falany *et al* (2000). Hepatic expression of an incorrectly spliced and untranslatable form of hSULT4A1 mRNA was described. This type of aberrant splicing may also be occurring in the testes of zebrafish. If the included intron was of sufficient length, that could explain why no amplicon was observed after conventional PCR using full length SULT4A1 primers (Fig. 2b). If intron 1 were included in the transcript, then the amplicon would increase from 860 to 6239 bases. That would be too long for amplification under the PCR conditions utilized.

Previous studies have shown the brain to be the primary site of SULT4A1 expression in humans and rats (Falany, 2000; Liyou, 2003). As expected, SULT4A1 expression was observed at high levels in the brain of adult zebrafish. Interestingly, SULT4A1 expression was also observed in the adult zebrafish eye (Fig. 2a & 2b). This represents a previously unreported finding that may provide key insights into the function of SULT4A1. If SULT4A1 does indeed prove to play an important role in vertebrate vision, then this finding further solidifies the zebrafish as a model organism to study its function. Zebrafish have the ability to respond to light as early as 68 hpf and can track movement as early as 73 hpf (Easter and Nicola, 1996). The strong ocular expression of SULT4A1 may also account for its relatively rapid onset of expression in zebrafish embryos, where protein was detectable by immunoblotting as early as 72 hpf (Fig. 2d). This stands in contrast to rats, where significant levels of brain SULT4A1 mRNA were not detectable by Northern-blot analysis until post-natal day 21 (Falany, 2000). Significant retinal development occurs in rats postnatally, especially with regards to photoreceptors. Cones do not reach peak density until post-natal day 10 (Arango-Gonzalez, 2012). This stands in contrast to larval zebrafish

vision, in which cones develop early on and are the primary photoreceptor type during the first few days of eye development (Fadool and Dowling, 2008).

The ocular expression of SULT4A1 may help explain the observed up-regulation of 13 genes known to be involved in phototransduction. Although adult zebrafish express higher levels of SULT4A1 in the brain than in the eye, at 72 hpf the eyes are the largest neuronal structure in the developing larvae. The immediate cause of this increase in expression remains unclear. Either SULT4A1 KD leads to an increase in the overall number of photoreceptors in the retina, or the number of photoreceptors remains the same while phototransduction protein expression increases. Given the lack of any discernible change in gross eye morphology of SULT4A1 KD larvae at 72 hpf, the latter seems more likely. Further investigation of the retinal histology of SULT4A1 KD larvae is needed to address these possibilities.

An interesting aspect of the phototransduction up-regulation in the SULT4A1 KD larvae is that it appears to be cone-specific. Of the 13 up-regulated genes, 8 are either exclusively or primarily expressed in cone photoreceptors as compared to rod photoreceptors. Four are expressed in both cones and rods, and only 1 is primarily expressed in rods. OPN1LW2, OPN1MW1, OPN1SW1, and OPN1SW2 encode the cone-specific opsin photopigments and displayed the most statistically significant up-regulation in the RNA-seq analysis. In contrast the rod-specific photopigment, rhodopsin, was not significantly dis-regulated. Arr3, grk1b, and grk7a are also primarily cone genes whose expression was shown by RNA-seq to be up-regulated (Renninger, 2001; Wada, 2006). The only rod-specific gene shown to be up-regulated was the transducin alpha subunit gnat1 (Nelson, 2008). The cone counterpart of gnat1, gnat2, was also up-regulated (Table 2). Larval zebrafish vision is dominated by cones (Fadool and Dowling, 2008), which may account for the disproportionate number of cone genes shown to be up-regulated by SULT4A1 KD.

Previous studies have shown that SULT4A1 does not bind the SULT cofactor product, 3',5'-phosphoadenosine (PAP) the same way as other SULTs (Allali-Hassani, 2007). Combined with the lack of detectable sulfation activity with a wide range of known SULT substrates, it is possible that SULT4A1 may act as an allosteric regulator of another protein rather than as a catalytically active SULT (Falany, 2000; Allali-Hassani, 2007). Therefore, deficits in SULT4A1 expression as seen in KD embryos could lead to dramatic changes in a cellular pathway whose activity is modulated by SULT4A1. Whether SULT4A1 is directly involved in phototransduction or some other neuronal process less specific to retinal and pineal tissue remains to be determined. However, given SULT4A1's wide distribution in the rat central nervous system (Liyou, 2003), the latter seems more likely. It is also possible that SULT4A1 may be expressed in the retinal ganglion cells, whose axons make up the optic nerve. While phototransduction was by far the most significantly affected cellular process in this study, this may be due to the rapid development of vision in the zebrafish larvae. Vision and the ability to react to visual stimuli play a prominent role in the development of zebrafish larvae (Easter and Nicola, 1996). Consequently, the eyes of a 72 hpf larva are disproportionately large compared to the rest of the body than those of an adult zebrafish. In contrast to KD larvae, adult SULT4A1-deficient zebrafish may present with more significant changes in different pathways such as circadian rhythm or CREB signaling in neurons (Table 3). To investigate the effects of SULT4A1 knockout in adult zebrafish, a mutant zebrafish line with inheritable deficits in SULT4A1 expression/function is under development. This study is the first to identify a cellular process whose regulation appears to be associated with SULT4A1 expression. The observation that KD of SULT4A1 expression in zebrafish larvae affects expression of genes in phototransduction represents the first possible function of this conserved orphan SULT. Characterization of visual responses and cone function in the KD larvae may identify the affected downstream visual signaling pathways.

DMD Fast Forward. Published on February 19, 2014 as DOI: 10.1124/dmd.114.057042
This article has not been copyedited and formatted. The final version may differ from this version.

AUTHORSHIP CONTRIBUTIONS

Participated in research design: Crittenden, Kraft, Parant, and Falany

Conducted experiments: Crittenden and Thomas

Contributed new reagents or analytic tools: Ethen, Wu, Parant, and Falany

Performed data analysis: Crittenden, Chen, Kraft, Parant, and Falany

Wrote or contributed to the writing of the manuscript: Crittenden, Chen, and Falany

REFERENCES

Allali-Hassani A, Pan PW, Dombrovski L, Najmanovich R, Tempel W, Dong A, Loppnau P, Martin F, Thonton J, Edwards AM, Bochkarev A, Plotnikov AN, Vedadi M, and Arrowsmith CH (2007) Structural and chemical profiling of the human cytosolic sulfotransferases. *PLoS Biol.* **5(5):** 1063-1078

Arango-Gonzalez B, Szabó A, Pinzon-Duarte G, Lukáts A, Guenther E, and Kohler K (2012) In Vivo and In Vitro Development of S- and M-Cones in Rat Retina. *Invest Ophthalmol Vis Sci*. **51(10):** 5320-5327

Benjamini Y and Hochberg Y (1995). Controlling the False Discovery Rate: A Practical and Powerful Approach to Multiple Testing. *J Roy Statist Soc Ser B* **57(1):** 289–300.

Blanchard RL, Freimuth RR, Buck J, Weinshilboum RM, and Coughtrie MW (2004) A proposed nomenclature system for the cytosolic sulfotransferase (SULT) superfamily. *Pharmacogenetics* **14(3):** 199-211

Bradford MM (1976) A rapid and sensitive method for the quantitation of microgram quantities of protein utilizing the principle of protein-dye binding. *Anal Biochem* **72**: 248–54

Das T, Payer B, Cayouette M, and Harris WA (2003) In Vivo time-lapse imaging of cell divisions during neurogenesis in the developing zebrafish retina. *Neuron* **37:** 597-609

Draper BW, Morcos PA, and Kimmel CB (2001) Inhibition of zebrafish fgf8 pre-mRNA splicing with morpholino oligos: a quantifiable method for gene knockdown. *Genesis* **30:** 154-156

Easter SS and Nicola GN (1996) The development of vision in the zebrafish. *Dev Biol* **180:** 646-663

Fadool JM and Dowling JE (2008) Zebrafish: a model system for the study of eye genetics. *Prog Retin Eye Res* **27(1):** 89-110

Falany CN, Kerl EA (1990) Sulfation of minoxidil by human liver phenol sulfotransferase. *Biochem Pharmacol* **40(5):** 1027-32

Falany CN, Xie X, Wang J, Ferrer J, and Falany JL (2000) Molecular cloning and expression of novel sulphotransferase-like cDNAs from human and rat brain. *Biochem J* **325:** 857-864

Grunwald DJ, Kimmel CB, Westerfield M, Walker C, and Streisinger G (1988) A neural degeneration mutation that spares primary neurons in the zebrafish. *Dev Biol* **126:** 115-128

Liu T, Bhuiyan S, Liu M, Sugahara T, Sakakibara Y, Suiko M, Yasuda S, Kakuta Y, Kimura M, Williams FE, and Liu M (2010) Zebrafish as a model for the study of the Phase II cytosolic sulfotransferases. *Curr Drug Metab* **11:** 538-546

Liyou NE, Buller KM, Tresillian MJ, Elvin CM, Scott HL, Dodd PR, Tannenberg AEG, and McManus ME (2003) Localization of a brain sulfotransferase, SULT4A1, in the human and rat brain: an immunohistochemical study. *J Histochem Cytochem* **51(12):** 1655-64

Mitchell DJ and Minchin RF (2009) Cytosolic aryl Sulfotransferase 4A1 interacts with the peptidyl prolyl cis-trans isomerase Pin1. *Mol Pharmacol* **76:** 388-395

Mitchell DJ, Butcher NJ, and Minchin RF (2011) Phosphorylation /dephosphorylation of human SULT4A1: role of Erk1 and PP2A. *Biochim Biophys Acta* **1813(1):** 231-237

Mortazavi A, Williams BA, McCue K, Schaeffer L, and Wold B (2008) Mapping and quantifying mammalian transcriptomes by RNA-Seq. *Nature* **5:** 621-8.

Nelson SM, Frey RA, Wardwell SL, and Stenkamp DL (2008) The developmental sequence of gene expression within the rod photoreceptor lineage in embryonic zebrafish. *Dev Dyn* **237(10):** 2903-2917

Ramsey TL, Meltzer HY, Brock GN, Mehrotra B, Jayathilake K, Bobo WV, and Brennan MD (2011) Evidence for a SULT4A1 haplotype correlating with baseline psychopathology and atypical antipsychotic response. *Pharmacogenomics* **12(4)**: 471-480

Renninger SL, Gesemann M, and Neuhauss SCF (2011) Cone arrestin confers cone vision of high temporal resolution in zebrafish larvae. *Eur J Neurosci* **33:** 658-667

Trapnell C, Pachter L, and Salzberg SL (2009) TopHat: discovering splice junctions with RNA-Seq. *Bioinformatics* **25**: 1105-1111.

Trapnell C, Williams BA, Pertea G, Mortazavi AM, Kwan G, van Baren MJ, Salzberg SL, Wold B, Pachter L (2010) Transcript assembly and quantification by RNA-Seq reveals unannotated transcripts and isoform switching during cell differentiation. *Nature Biotechnology* **28(5):** 511-5

Wada Y, Sugiyama J, Okano T, and Fukada Y (2006) GRK1 and GRK7: unique cellular distribution and widely different activities of opsin phosphorylation in zebrafish rods and cones. *J Neurochem* **98:** 824-837

Wang ET, Sandberg R, Luo S, Khrebtukova I, Zhang L, Mayr C, Kingsmore SF, Schroth GP, and Burge CB (2008) Alternative isoform regulation in human tissue transcriptomes. *Nature* **456:** 470-6.

Wang Z, Gerstein M, Snyder M (2009) RNA-Seq: a revolutionary tool for transcriptomics. *Nat Rev Genet* **10:** 57-63

Xing Y, Yu T, Wu YN, Roy M, Kim J, Lee C (2006) An expectation-maximization algorithm for probalisitic reconstructions of full-length isoforms from splice graphs. *Nucleic Acids Res* **34:** 3150-3160.

Yasuda S, Liu C, Takahashi S, Suiko M, Chen L, Snow R, and Liu M (2005) Identification of a novel estrogen-sulfating cytosolic SULT from zebrafish: Molecular cloning, expression, characterization, and ontogeny study. *Biochem Biophys Res Commun* **330:** 219-225

FOOTNOTES

This work was supported by the National Institute of Mental Health [Grant: R21MH095946].

DMD Fast Forward. Published on February 19, 2014 as DOI: 10.1124/dmd.114.057042
This article has not been copyedited and formatted. The final version may differ from this version.

FIGURE LEGENDS

Figure 1: Amino acid sequence homology between human and zebrafish SULT4A1.

Sequences are 86.9% identical and 91.9% similar. Asterisks indicate conserved amino acids. Periods indicate a changed residue that maintains the same electrochemical properties. Key conserved features are highlighted in black and include the active site His (residue 111), the KXXFTVXXXE dimerization domain (residues 254-263), and the TYPKSGT PAPS binding domain (residues 52-58).

Figure 2: SULT4A1 expression and MO knockdown in zebrafish.

A. Quantitative real-time PCR. Relative expression levels were analyzed using the ΔCt method and normalized to endogenous expression of 18s RNA. Error bars indicate standard error of the mean. Brain ($2.54e^{-4}$ +/- $4.24e^{-5}$). Eye ($8.45e^{-5}$ +/- $1.01e^{-5}$). Intestine ($1.75e^{-5}$ +/- $5.35e^{-6}$). Liver ($7.7e^{-6}$ +/- $1.48e^{-6}$). Testes ($8.69e^{-5}$ +/- $8.09e^{-6}$). **B.** Qualitative PCR of SULT4A1 message in adult AB zebrafish brain, eye, intestine, liver, and testes using full-length primers (forward: 5'-atggcggaaagcgaggtgga-3'; reverse: 5'-ctgctttacaggataaagtc-3'). **C.** Immunoblot of zebrafish brain and eye lysate using anti-human SULT4A1 polyclonal antibody. Each lane was loaded with 396 µg lysate. Arrows indicate molecular weight. **D.** Immunoblot of SULT4A1 in control and knockdown embryos at 72 hpf using an anti-human SULT4A1 polyclonal antibody. Each lane was loaded with 173 µg.

Figure 3: qPCR verification of differentially expressed phototransduction genes observed in RNA-seq data at 72 hpf.

SuperScript III was used to generate cDNA from total RNA. Message level was determined on a 7900HT Sequence Detection System using pre-designed TaqMan Gene Expression Assays. Values represent average relative mRNA expression (n=3) +/- the standard error of the mean. **A.** SULT4A1: SCM (1.00 +/-

0.31). SULT4A1 MO (0.15 +/- 0.04). P = 0.0253. **B.** rrh: SCM (1.00 +/- 0.12). SULT4A1 MO (1.24 +/- 0.23). P = 0.1917. **C.** guca1e: SCM (1.00 +/- 0.17). SULT4A1 MO (1.52 +/- 0.26). P = 0.0822. **D.** grk1b: SCM (1.00 +/- 0.14). SULT4A1 MO (1.43 +/- 0.11). P = 0.0392. **E.** OPN1MW1: SCM (1.00 +/- 0.10). SULT4A1 MO (2.15 +/- 0.22). P = 0.0047. *p<0.05 as compared to SCM-injected embryos.

Figure 4: Normal development of WT and KD zebrafish embryos.

Larvae were immobilized in 2% methyl cellulose and visualized using a Nikon AZ100 microscope. **A.** 48 hpf Control. **B**. 48 hpf SULT4A1 MO. **C**. 72 hpf Control. **D**. 72 hpf SULT4A1 MO. **E.** 120 hpf Control. **F.** 120 hpf SULT4A1 MO.

Table 1: Sequence homology of SULT4A1 across different vertebrate species.

AA changed denotes the number of amino acid residues that differ from the human isoform of SULT4A1. Similar AA denotes the number of amino acid residues that differ from the human isoform of SULT4A1, but maintain the same electrochemical properties. Numbers in parentheses indicate GenBank accession number.

Species	Total AA	AA Changed	% Identical	Similar AA	% Similar
Human (CAG30474)	284				
Rabbit (NP_001076173)	284	4	98.59	2	99.3
Rat (NP_113829)	284	6	97.89	4	98.59
Finch (NP_001232743)	284	16	94.37	7	97.54
Frog (NP_001087553)	284	31	89.08	18	93.66
Zebrafish (NP_001035334)	284	37	86.97	23	91.9

Table 2: Summary of affected genes involved in phototransduction. Embryos injected with SCM or SULT4A1 MO were subjected to gene expression profiling using RNA-seq. P-Values were determined using ANOVA.

DMD Fast Forward. Published on February 19, 2014 as DOI: 10.1124/dmd.114.057042
This article has not been copyedited and formatted. The final version may differ from this version.

Protein	Gene	Fold Change	p Value	Localization
Sulfotransferase family 4A member 1	SULT4A1	-2.15	<0.0001	
Rhodopsin	RHO	1.17	0.8233	Rod
G protein alpha transducing activity polypeptide 1	GNAT1	2.09	<0.0001	Rod
G protein alpha transducing activity polypeptide 2	GNAT2	3.35	<0.0001	Cone
G-protein-coupled receptor kinase 7a	grk7a	3.33	<0.0001	Cone
opsin 1, long-wave-sensitive, 2	OPN1LW2	2.31	<0.0001	Cone
opsin 1, medium-wave-sensitive, 2	OPN1MW1	4.56	<0.0001	Cone
opsin 1, short-wave-sensitive, 1	OPN1SW1	3.62	<0.0001	Cone
opsin 1, short-wave-sensitive, 2	OPN1SW2	3.29	<0.0001	Cone
G protein-coupled receptor kinase 1b	grk1b	4.27	<0.0001	Cone
Arrestin 3, retinal	ARR3	1.87	<0.0001	Cone
guanine nucleotide binding protein (G protein), gamma transducing activity polypeptide 2b	gngt2b	3.24	<0.0001	Both
Phosducin b	pdcb	2.76	<0.0001	Both
Guanylate cyclase activator 1e	guca1e	4.39	0.00018	Both
Cyclic nucleotide gated channel beta 1a	cngb1a	3.51	<0.0001	Both

Table 3: Gene ontology of transcripts affected by SULT4A1 knockdown.

Following collection of RNA-seq data, Ingenuity Pathway Analysis was used to group affected genes into functional pathways and generate p-values.

Pathway	P-value	Genes
Phototransduction Pathway	2.48E-16	ARR3a, cngb1a, guca1e, GNAT1, GNAT2, gngt2b, OPN1LW2, OPN1MW1, OPN1SW1, OPN1SW2, grk1b, grk7a, pdcb
LXR/RXR Activation	4.19E-3	APOA4, CYP7A1, MMP9, CETP
Circadian Rhythm Signaling	1.42E-2	PER1, NR1D1
CREB Signaling in Neurons	1.43E-2	GNAT1, GRM1, NAT2, OPN1SW

Figure 1


hSULT4A1 MAESEAETPSTPGEFESKYFEFHGVRLPPFCRGKMEEIANFPVRPSDVWI 50
zSULT4A1 MAESEVDTPSTPIEYESKYFEHHGVRLPPFCRGKMDEIANFSLRSSDIWI 50
hSULT4A1 VTYPKSGTSLLQEVVYLVSQGADPDEIGLMNIDEQLPVLEYPQPGLDIIK 100
zSULT4A1 VTYPKSGTSLLQEVVYLVSQGADPDEIGLMNIDEQLPVLEYPQPGLEIIQ 100
hSULT4A1 ELTSPRLIKSHLPYRFLPSDLHNGDSKVIYMARNPKDLVVSYYQFHRSLR 150
zSULT4A1 ELTSPRLIKSHLPYRFLPSAMHNGEGKVIYMARNPKDLVVSYYQFHRSLR 150
hSULT4A1 TMSYRGTFQEFCRRFMNDKLGYGSWFEHVQEFWEHRMDSNVLFLKYEDMH 200
zSULT4A1 TMSYRGTFQEFCRRFMNDKLGYGSWFEHVQEFWEHRMDSNVLFLKYEDMY 200
hSULT4A1 RDLVTMVEQLARFLGVSCDKAQLEALTEHCHQLVDQCCNAEALPVGRGRV 250
zSULT4A1 KDLGTLVEQLARFLGVSCDKAQLESLVESSNQLIEQCCNSEALSICRGRV 250
hSULT4A1 GLWKDIFTVSMNEKFDLVYKQKMGKCDLTFDFYL 284
zSULT4A1 GLWKDVFTVSMNEKFDVIYRQKMAKSDLTFDFIL 284

Figure 2

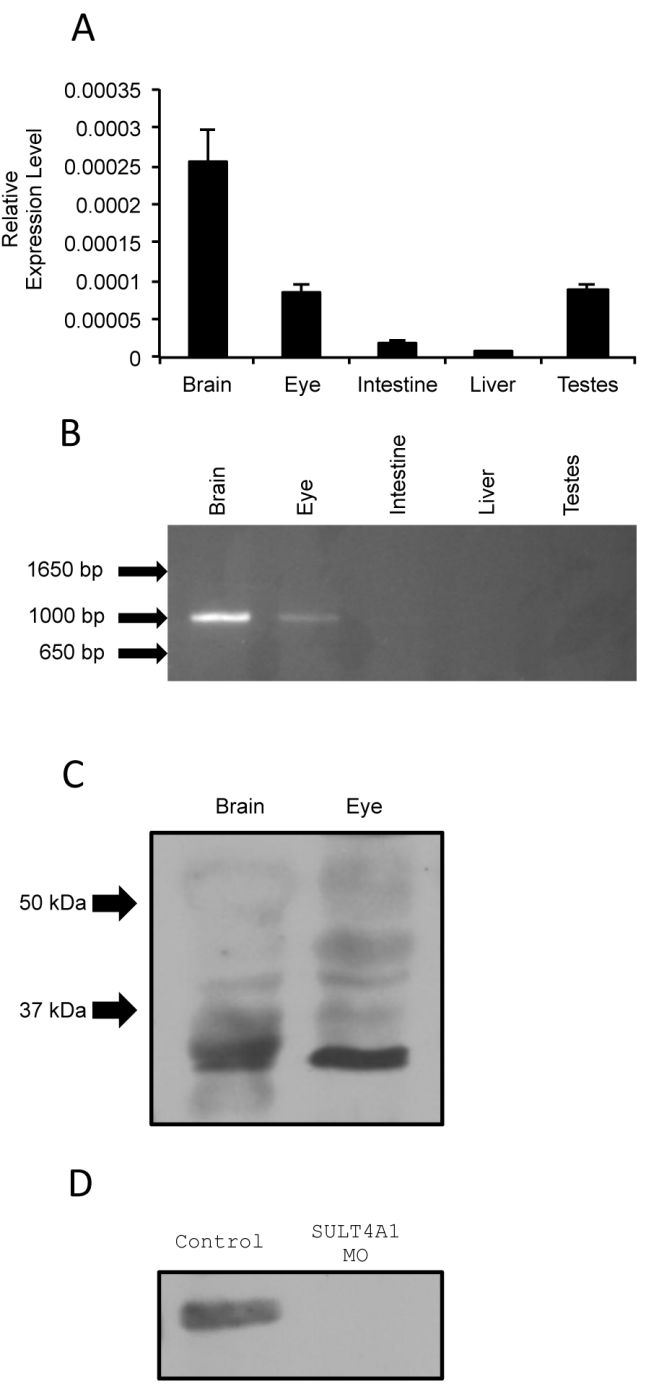
A
Relative Expression Level
0.00035
0.0003
0.00025
0.0002
0.00015
0.0001
0.00005
0
Brain
Eye
Intestine
Liver
Testes
B
Brain
Eye
Intestine
Liver
Testes
1650 bp
1000 bp
650 bp
C
Brain
Eye
50 kDa
37 kDa
D
Control
SULT4A1 MO

Figure 3

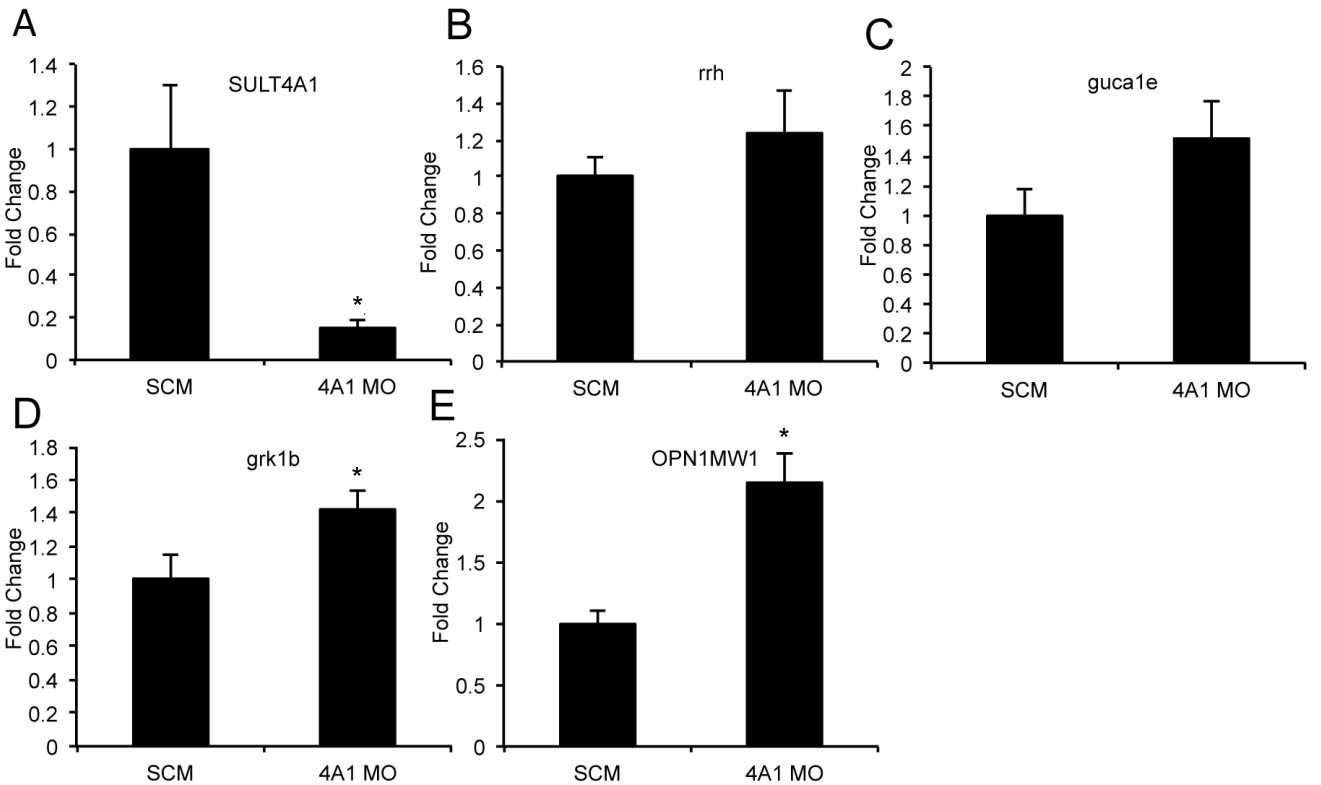
A
SULT4A1
Fold Change
1.4
1.2
1
0.8
0.6
0.4
0.2
0
*
SCM
4A1 MO
B
rrh
Fold Change
1.6
1.4
1.2
1
0.8
0.6
0.4
0.2
0
SCM
4A1 MO
C
guca1e
Fold Change
2
1.8
1.6
1.4
1.2
1
0.8
0.6
0.4
0.2
0
SCM
4A1 MO
D
grk1b
Fold Change
1.8
1.6
1.4
1.2
1
0.8
0.6
0.4
0.2
0
*
SCM
4A1 MO
E
OPN1MW1
Fold Change
2.5
2
1.5
1
0.5
0
*
SCM
4A1 MO

Figure 4